

Title	Growth process of cubic boron nitride films in bias sputter deposition
Author(s)	Yamada, Yukiko; Tatebayashi, Yoshinao; Tsuda, Osamu; Yoshida, Toyonobu
Citation	Thin Solid Films, 295(1-2): 137-141
Issue Date	1997-02-28
Type	Journal Article
Text version	author
URL	http://hdl.handle.net/10119/4968
Rights	NOTICE: This is the author's version of a work accepted for publication by Elsevier. Yukiko Yamada, Yoshinao Tatebayashi, Osamu Tsuda and Toyonobu Yoshida, Thin Solid Films, 295(1-2), 1997, 137-141, http://dx.doi.org/10.1016/S0040-6090(96)09285-1
Description	

Growth process of cubic boron nitride films in bias sputter deposition

Yukiko Yamada*, Yoshinao Tatebayashi, Osamu Tsuda and Toyonobu Yoshida

Department of Metallurgy and Materials Science, Graduate School of Engineering, The University of Tokyo, 7-3-1 Hongo Bunkyo-ku Tokyo 113 Japan.

*Research Fellow of Japan Society for the Promotion of Science

Abstract

Intending to study phase evolution of cubic boron nitride (*c*BN) films during RF bias sputter deposition, surfaces of the *c*BN films in different growth stages were examined systematically. Argon content at the film surface increased during the deposition of initial sp^2 bonded layer growth, and saturated at about 1.5 at.%, and remained constant after the formation and growth of cubic phase, accompanied with an increase of compressive stress up to 5 GPa. This increase of stress is confirmed to be the result of averaging film stress over the double-layered *c*BN film, that is, over low-stressed initial layer and high-stressed cubic layer. Atomic force microscope (AFM) observations in tapping mode revealed self-affine fractal nature and kinetic roughening of film surface during the growth, and root mean square (rms) roughness changed from 0.3 nm of an initial layer, to 0.9 nm accompanied with peculiar surface smoothing at the initial stage of *c*BN formation. Moreover, the evolution of the surface roughness was clearly characterized by the change of modes in each growth process, that is, an initial layer growth stage, a transition stage, and a cubic layer growth stage.

1. Introduction

Cubic BN films have been successfully synthesized by numbers of PVD and CVD processes in these several years[1]. An important common feature of these processes can be characterized by bombardments of sufficient amount of energetic particles to growing surface of depositing film. Therefore a role of energetic particles in formation of *c*BN is in great interest. It has been revealed that *c*BN formation is momentum-driven[2], but the exact role of these energetic particles remains unknown. Another mystery in *c*BN film growth is the presence of an initial sp^2 bonded layer with considerable thickness. Recent results in cross sectional TEM observation of *c*BN films prepared by ion beam assisted evaporation, clearly showed layered structure of *a*BN, oriented *t*BN and *c*BN [3, 4]. The growth of sp^2 bonded phase preceding the growth of sp^3 bonded phase was also observed by several groups[5, 6, 7, 8]. Considering these results, two-stage growth process is speculated as a general growth process of a *c*BN film, and it seems that not only the depositing particle conditions but also growing surface has an important role in the formation of *c*BN.

We therefore felt a great significance in studying surface conditions of growing *c*BN film, especially where the cubic phase formation occurs. We report on our results of surface analyses and film stress measurements of *c*BN films deposited on silicon substrates by RF bias sputtering, and discuss the difference in surface evolution during the growing process.

2. Experimental

Cubic BN films were deposited on $32 \times 32 \text{ mm}^2$ sized p-type $\langle 100 \rangle$ oriented silicon wafer by RF bias sputtering with a sintered *h*BN target. Detail

descriptions of our apparatus was reported elsewhere[5]. Deposition conditions are shown in Table 1. All depositions were carried out after presputtering target and substrate for 15 minutes in “presputtering condition”, with a shutter between electrodes closed. Deposition conditions were maintained constant except for deposition times ranging from 30 s to 300 s. Maximum thickness of the films measured by cross sectional scanning electron microscope (SEM) image was about 110 nm, and all the samples stayed adhered to the substrates without peeling off.

Phase identification of deposited films were mainly accomplished by transmission micro FTIR spectrometer (FT/IR-700, JASCO). Measurements with a spot size of $200 \times 200 \mu\text{m}^2$ were carried out through the films with silicon substrates, as soon as they were taken out from deposition chamber. Composition and chemical state of the deposited film surface were examined by an X-ray photoelectron spectrometer (XPS-7000, Rigaku Denki) with an X-ray source of nonmonochromatized Mg K_{α} radiation (1253.6 eV). The analyzer was operated at 15 eV pass energy providing 1.2 eV resolution. Binding energy was calibrated by C1s line at 284.6 eV. No surface treatment of the films was done before these measurements.

Film stress was evaluated by measuring the substrate curvature before and after deposition, and employing it to Stoney’s equation modified for plate geometry[9, 10]. Substrate curvature was measured by a surface profilometer (SURFCOM 470A, Tokyo Seimitsu). Reduced elastic modulus of Si (100) plane was cited from ref.11.

Surface morphology of the deposited films were examined by tapping mode AFM (Nanoscope III, Digital Instruments) under ambient condition. Humidity

around the apparatus was about 40 % during the observations. In contrast with contact mode AFM, observed images were clear and reproducible due to its small imaging force and absence of lateral force. AFM tips made of silicon with tip radius of 5 to 10 nm and half cone angle of 18 degree (TTAFM, NANOSENSORS) were used. Drive frequency of the tip was around 300 kHz, and free oscillation amplitude was set to approximately 80 nm. Careful attention was paid to reproducibility of images observed through many scans and with different tips in order to avoid image distortion by damaged tips.

3. Results and Discussions

IR absorbances of sp^3 bonded phase (around 1080 cm^{-1}) and sp^2 bonded phase (around 1380 cm^{-1}) of the films deposited with different deposition times are shown in Fig.1. It shows that in initial growth stage, sp^2 bonded phase grows until the critical thickness, and then cubic phase forms and grows in a single phase. The cubic phase appears to be formed at 75 s, which was confirmed by the IR spectra; the peak around 1080 cm^{-1} was not so clear, but faint increase of absorbance was apparent. The thickness of the films deposited over 120 s were measurable from SEM images. Assuming time-linear growth of cubic phase and extrapolating these measured thickness to 75 s, where cubic phase forms, initial layer thickness of 50 nm was estimated. Approximate deposition rate of the initial layer, 0.7 nm/s, seems to be considerably higher than the deposition rate of cubic phase, 0.3 nm/s.

XPS analyses revealed that N/B atomic ratio of the films were nearly stoichiometric throughout the samples regardless of the deposition time. Beside boron and nitrogen peaks, argon, carbon and oxygen associated peaks were

observed in every sample. Carbon and oxygen are considered as surface contamination while handling in air. Argon in the film is derived from the ion bombardment during the film growth. Figure 2 shows argon content at the surface of the films in different growth stages. Argon content increased as initial layer grew, and saturated around where sp^3 bonded cubic phase formation occurred. The amount of argon embedded in surface seems to remain unchanged at about 1.5 at. % during the cubic phase growth. McKenzie *et al.* [10] have reported difference in argon concentration between *c*BN film (1 % argon concentration) and *h*BN film (undetectable) prepared by ion plating, and mentioned that dense atomic packing of *c*BN entraps argon more easily than the oriented *h*BN layer. The same tendency was observed in our case, and our result additionally suggests some change in sp^2 bonded phase structure during the initial layer growth. Its structure seems to have changed into more argon-trappable, pre-cubic, dense structure. To identify phase present in growing front, energy loss peaks from B1s core level peak were examined. For films with no IR absorbance around 1080 cm^{-1} (deposition time $t = 30\sim 60\text{ s}$), additional π plasmon loss peak at about 9 eV higher binding energy from the core level peak was observed. For films in state of initial cubic phase formation on sp^2 bonded layer ($t = 75\sim 90\text{ s}$) the peak was observed faintly. This result suggests that in this growth stage, sp^2 bonded phase and sp^3 bonded phase may coexist at the growing surface. The peak was not observed from the films containing high amount of cubic phase ($t = 120\sim 300\text{ s}$). Thus surfaces of these films are considered to be completely covered with *c*BN.

Figure 3 (a) shows evolution of compressive stress with increase in film thickness. At a glance, the compressive stress in cubic phase seems to increase as

cubic phase grows. However, this increase is the result of evaluating film stress over the double-layered *c*BN film thickness, that is, over low-stressed initial layer and high-stressed cubic layer. Figure 3 (b) shows evolution of calibrated film stress using the thickness of cubic layer alone instead of a total film thickness. This result clearly shows that cubic layer in films are in equivalent highly compressive stressed state independent of their thickness.

Figure 4 shows tapping mode AFM images of *c*BN films in different growth stages. Figure 4 (a) is a surface image of an initial sp^2 bonded layer (deposition time $t = 45$ s). Likewise, (b) and (c) correspond to those of the films just after the cubic phase nucleated on the initial layer ($t = 90$ s) and after the surface was covered with cubic phase ($t = 300$ s) respectively. Grains of size about 20~40 nm were observed in every sample which is close to the size of *c*BN crystallites measured from transmission electron microscopy. This result suggests concurrent nucleation of *c*BN during the growth.

Quantitative analysis of surface roughness observed in AFM image could be done by a scaling analysis of root mean square (rms) roughness R_{rms} . Calculation of a scale dependent rms roughness using AFM height data was done by a method described in ref. 12. Referring to Westra *et al.*'s work[13], when the average radius of the major features in observed AFM image is five times larger than the radius of AFM tip, decrease in rms roughness by distortion of the image is less than 2 %. The smallest average radius of an AFM image observed in this experiment was about 150 nm and the nominal tip radius was 5 to 10 nm. Since the AFM images of each samples were reproducible through many scans and with different tips, we considered that the tip damage was small enough so that decrease in calculated rms roughness by image distortion was less than 2 %.

Figure 5 shows the scale dependent rms roughness of the films in Fig. 4. All curves are separated into two regions, scale-dependent part and scale-independent part. The scale-independent rms roughness estimated from a large scale part of the curve in Fig. 5 would be “the rms roughness”, which we can use as a representative value when we compare the surface roughness between different samples. It has recently been revealed that in some films when the scale is small enough, fractal nature of the surface roughness becomes noticeable[14, 15], and the rms roughness depends on its scan area size. This scale-dependent rms roughness $R_{\text{rms}}(L)$ is dependent on the scale L according to a power law of $R_{\text{rms}}(L) \propto L^{\alpha}$, where α is called roughness exponent[16]. The value of α can be estimated from the slope of a scale-dependent part in the curve, and α was approximately 0.6 for the films in cubic phase growth stage. For the films in initial layer growth stage and transition stage, α ranged from 0.3 to 0.6. Roughness exponent α in the range of $0 < \alpha < 1$ suggests anisotropic scaling, and BN film surfaces are thus identified as self-affine fractal[16]. Similar analyses of the films prepared by vapor deposition[17,18] and the films sputtered by ion beam[15] often result in self-affine fractal, and in this point *c*BN film was not an exception.

In Fig. 6, the scale-independent rms roughness R_{rms} estimated from the above method was plotted against deposition time. R_{rms} ranged from 0.3 nm to 0.9 nm while that of a pre-sputtered silicon substrate was below 0.2 nm. Kinetic roughening in the surface of growing *c*BN film and smoothing feature after cubic phase formation are apparent in Fig. 6. Scaling theory predicts a correlation of $R_{\text{rms}} \propto t^{\beta}$ for the films grown in a single process, where β is called growth exponent[16]. In our case, three regions (roughening-smoothing-roughening)

revealed in Fig. 6, corresponding to each growth stage, and β was unable to set to a single value throughout the *c*BN film growth. But for the film with deposition time longer than 150 s showed stable growth, and growth exponent β was estimated to be about 0.6. In this stage, *c*BN film is considered to grow in a single growing process, which is consistent with the result of roughness exponent mentioned above. The surface smoothing after cubic phase formation was also reported in the growth of *c*BN film in low pressure inductively coupled plasma enhanced chemical vapor deposition[6], and the surface smoothing and subsequent roughening during film growth was also reported in growth of polysilicon by low pressure chemical vapor deposition[19], though their origin is unknown. The difference in sputtering yield and growth speed between sp^3 bonded phase and sp^2 bonded phase might have resulted in this smoothing.

Above results are summarized as follows. The growth process of *c*BN film in RF bias sputter deposition can be separated into three stages. At an initial layer growth stage, sp^2 bonded layer grew in a single phase in relatively high deposition rate, 0.7 nm/s. The increase of argon content at a growing surface suggests concurrent structure change during growth of this layer. Compressive stress of the films in this stage was about 1 GPa and its evolution was hardly detectable. At a transition stage, where sp^2 bonded phase and sp^3 bonded phase seems to coexist, peculiar surface smoothing phenomenon was observed. At a cubic layer growth stage, single phase growth of sp^3 bonded phase was observed in both IR analysis and XPS analysis. This result is supported by consistency in argon content at growing surface and compressive stress. Moreover, scaling analysis of the surface roughness of the films in this growth stage resulted in a pair of scaling exponents, roughness exponent and growth exponent, and this

result should also be a consequence of a single growth process.

4. Conclusion

The evolution of surface chemistry, surface morphology and compressive stress during bias sputter deposition of *c*BN films were investigated. Different growth stages in *c*BN film growth could be clearly notified. At an initial stage, low-stressed sp^2 bonded layer grows with a concurrent change into argon-trappable, pre-cubic structure. At a transition stage from sp^2 bonded layer to sp^3 bonded layer, the surface is gradually covered with high-stressed *c*BN, and surface smoothing phenomenon occurs. At a cubic layer growth stage, high-stressed *c*BN grows in a single phase and a single growth process.

Acknowledgment

A part of this work is supported by Japan Society for the Promotion of Science.

The authors are grateful to Mr. H. Hamamatsu for his instruction on XPS measurement, to Prof. I. Yasui and Dr. F. Utsuno for kindly lending surface profilometer for the sample measurements, to Prof. K. Terashima and Mr. N. Yamaguchi for their instruction and suggestion on AFM operation, and to Dr. Y. Takamura for constructing program for calculating scale-dependent rms roughness from AFM height data.

References

- [1] T. Yoshida, *Diamond and Related Materials*, 5 (1996) 501
- [2] D. J. Kester and R. Messier, *J. Appl. Phys.*, 72 (1992) 504.
- [3] D. J. Kester, K. S. Ailey, R. F. Davis and K. L. More, *J. Mater. Res.*, 8 (1993) 1213.
- [4] D. J. Kester, K. S. Ailey, D. J. Lichtenwalner and R. F. Davis, *J.Vac.Sci.&Technol.*, A 12 (1994) 3074.
- [5] O. Tsuda, Y. Yamada, T. Fujii and T. Yoshida, *J.Vac.Sci.&Technol.*, A13 (1995) 2843.
- [6] T. Ichiki, S. Amagi and T. Yoshida, *J. Appl. Phys.*, 79 (1996) 4381.
- [7] D. L. Medlin, T. A. Friedmann, P. B. Mirkarimi, P. Rez, M. J. Mills and K. F. McCarty, *J. Appl. Phys.*, 76 (1994) 295.
- [8] S. Watanabe, S. Miyake, W. Zhou, Y. Ikuhara, T. Suzuki and M. Murakawa, *Appl. Phys. Lett.*, 66 (1995) 1478.
- [9] D. E. Fahnline, C. B. Masters and N. J. Salamon, *J.Vac.Sci.&Technol.*, A9 (1991) 2483.
- [10] D. R. McKenzie, W. D. McFall, W. G. Sainty, C. A. Davis and R. E. Collins, *Diamond and Related Materials*, 2 (1993) 970.
- [11] W. A. Brantley, *J. Appl. Phys.*, 44 (1973) 534.
- [12] A. Iwamoto and T. Yoshinobu, *Phys. Rev. B*, 48 (1993) 8282.
- [13] K. L. Westra and D. J. Thomson, *J.Vac.Sci.&Technol.*, B13 (1995) 344
- [14] A. Iwamoto, T. Yoshinobu and H. Iwasaki, *Phys. Rev. Lett.*, 72 (1994) 4025.
- [15] J. Krim, I. Heyvaert, C. Van Haesendonck and Y. Bruynseraede, *Phys. Rev. Lett.*, 70 (1993) 57.
- [16] See for example, A. -L. Barabasi and H. E. Stanley, Fractal concepts in surface growth, Cambridge University Press, Cambridge, First edn., 1995, p.20-37.
- [17] Y. -L. He, H. -N. Yang, T. -M. Lu and G. -C. Wang, *Phys. Rev. Lett.*, 69 (1992) 3770.
- [18] T. Yoshinobu, A. Iwamoto and H. Iwasaki, *Jpn. J. Appl. Phys.*, 33 (1994) L67.

[19] O. Vatel, E. Andre, F. Chollet, P. Dumas and F. Salvan,
J.Vac.Sci.&Technol., B12 (1994) 2037.

Table 1. Experimental Condition

Deposition condition		
target power		600 W
substrate bias voltage		-300 V
(substrate power	270 W)	
phase difference		0°
working pressure		2.1 Pa
sputtering gas		Ar
gas flow rate		40sccm
Presputtering condition		
target power		500 W
substrate power		100 W
(substrate bias voltage	-90 V)	

Figure captions

Fig. 1 FT-IR analysis of phase evolution in *c*BN film deposition process. IR absorbances of sp^3 phase ($\sim 1060\text{ cm}^{-1}$) and sp^2 phase ($\sim 1380\text{ cm}^{-1}$) in *c*BN films were determined in different growth stages.

Fig. 2 Argon content at the film surfaces of *c*BN films in different growth stages.

Fig. 3 The dependence of compressive stress on the phase evolution in *c*BN film deposition process. The stress was evaluated using (a) a whole film thickness and (b) a *c*BN layer thickness alone, respectively.

Fig. 4 Tapping mode AFM images of *c*BN films in different growth stages. Deposition times: (a) 45 s, (b) 90 s, (c) 300 s.

Fig. 5 Scale dependent rms roughness calculated from AFM height data of the films deposited for 45 s, 90 s and 300 s. Scan size : cross ($5\text{ }\mu\text{m} \times 5\text{ }\mu\text{m}$), circle ($2\text{ }\mu\text{m} \times 2\text{ }\mu\text{m}$), triangle ($1\text{ }\mu\text{m} \times 1\text{ }\mu\text{m}$), square ($500\text{ nm} \times 500\text{ nm}$) and rhombus ($300\text{ nm} \times 300\text{ nm}$).

Fig. 6 Time evolution of scale independent rms roughness during *c*BN film deposition process.

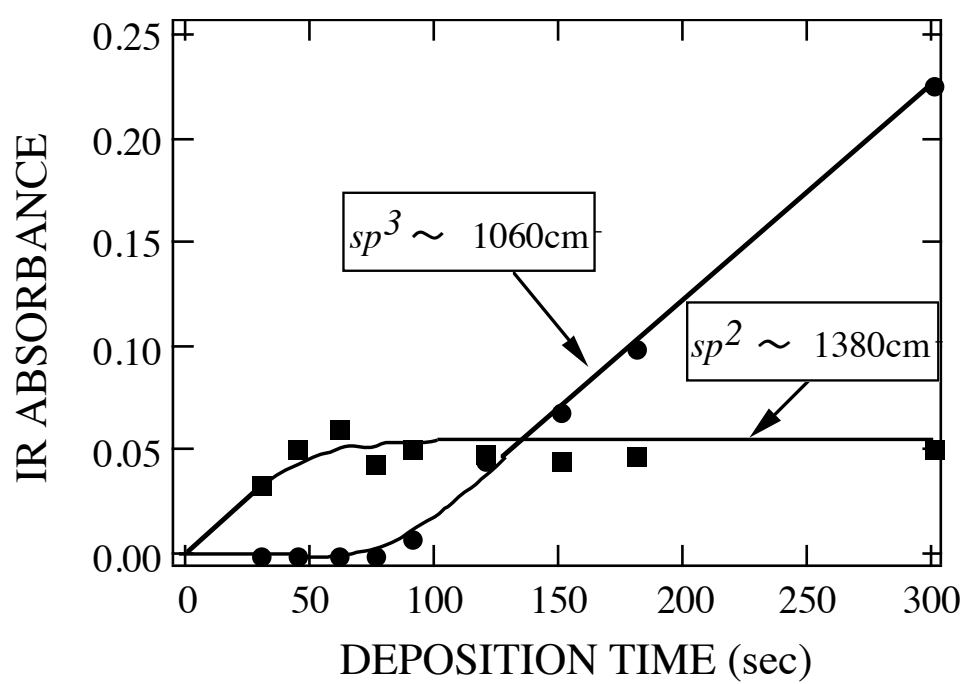


Figure 1

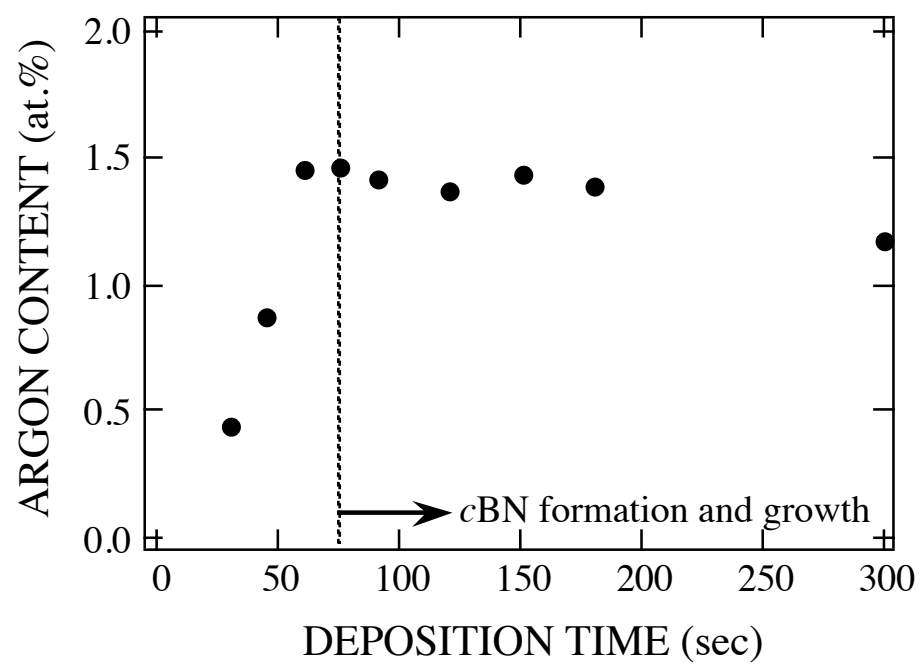


Figure 2

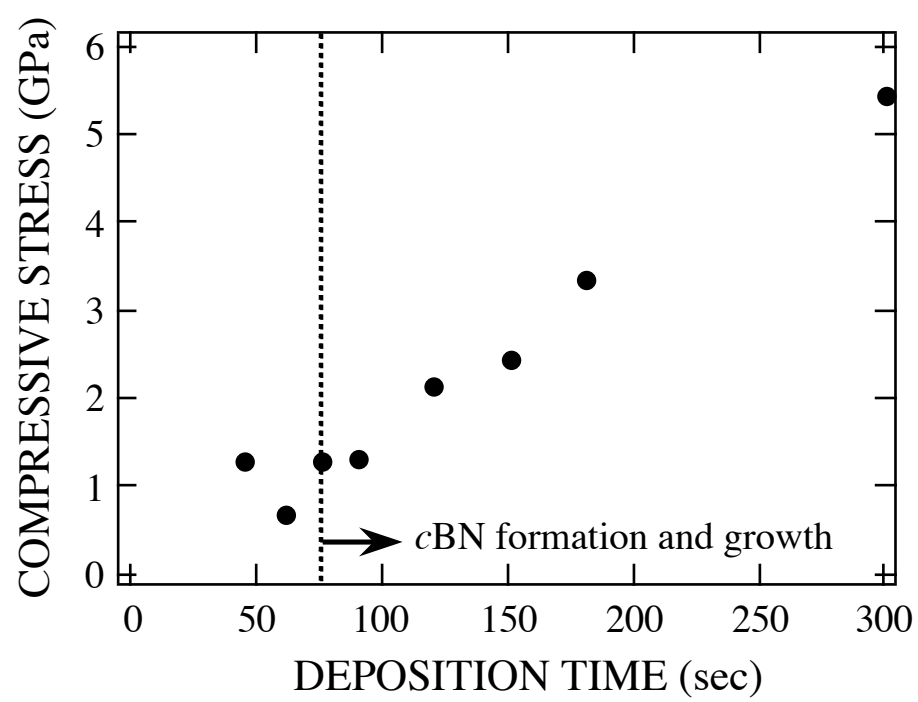


Figure 3(a)

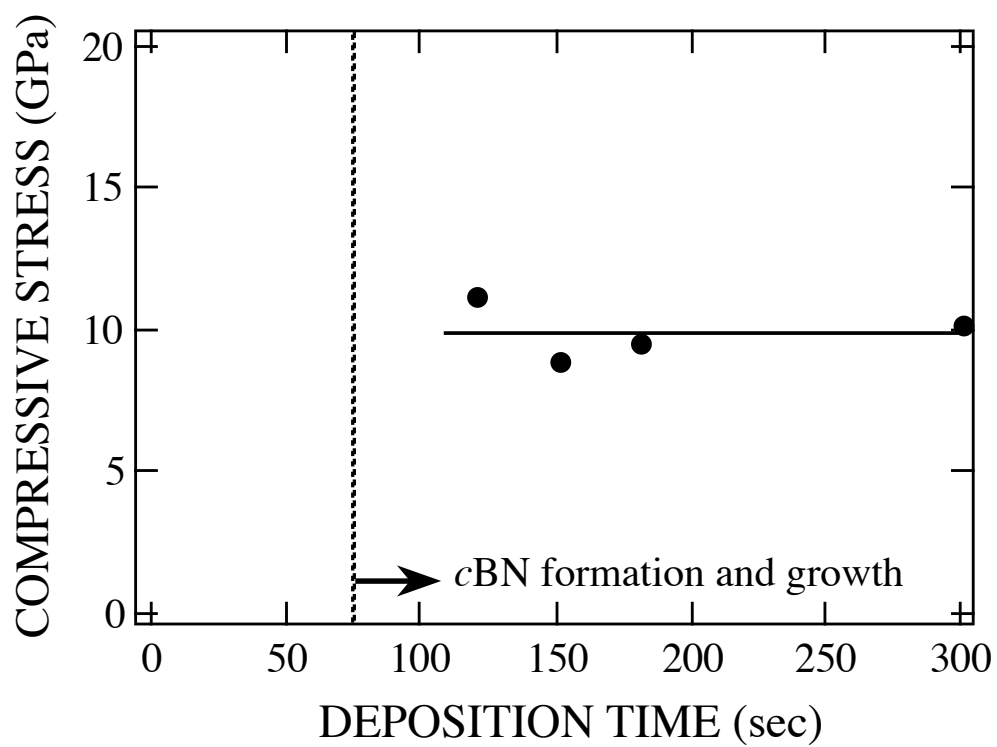


Figure 3(b)

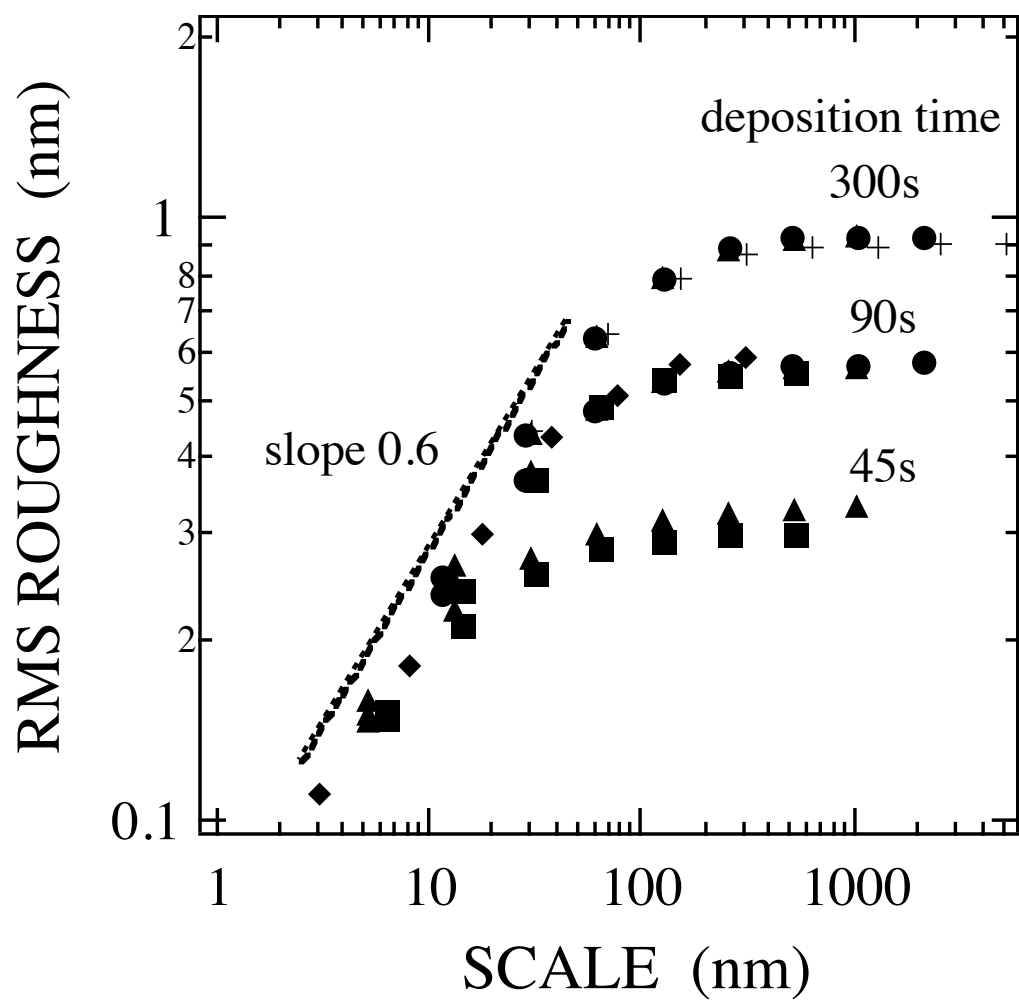


Figure 5

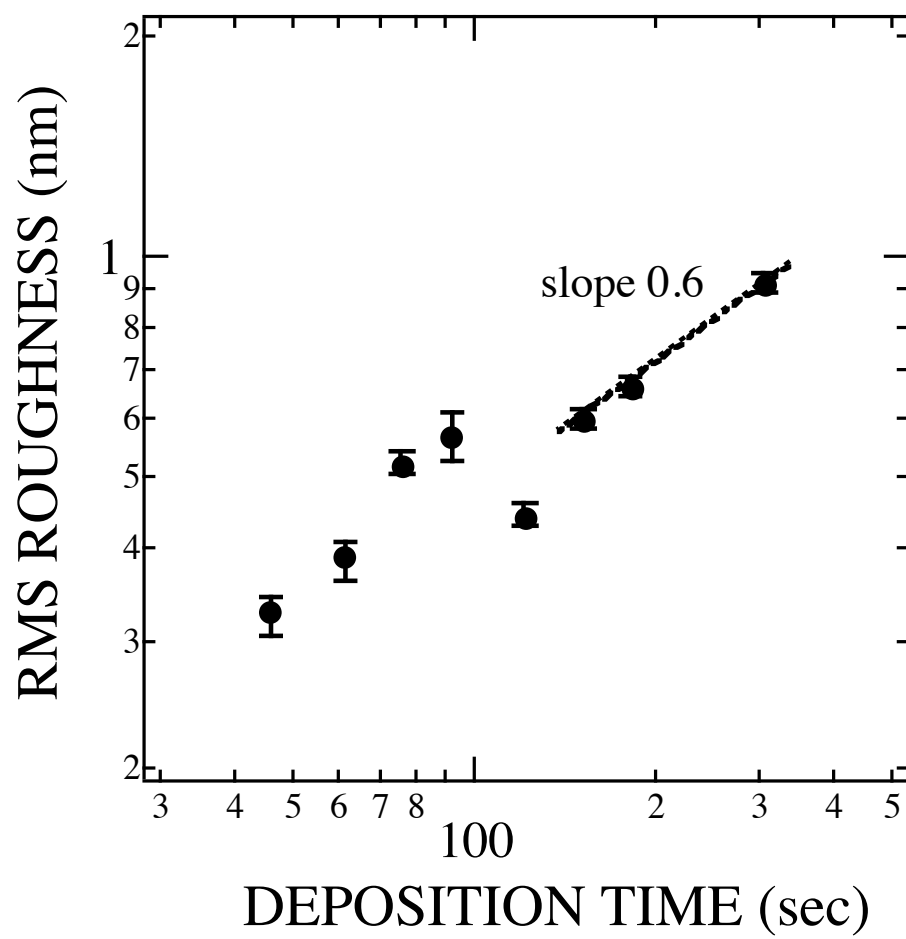


Figure 6